

STUDY OF COSMIC DUST PARTICLES ON BOARD LDEF
THE FRECOPA EXPERIMENTS AO138-1 AND AO138-2

J.C. Mandeville
ONERA/CERT Space Technology Department
BP 4025, 31055 Toulouse cedex France
Phone : 3361557117, Fax : 3361557172

Janet Borg
C.N.R.S Orsay Campus France
Phone : 3369415225, Fax : 3369415268

SUMMARY

Two experiments, within the French Cooperative Payload (FRECOPA) and devoted to the detection of cosmic dust have been flown on the Long Duration Exposure Facility (LDEF), launched in April 1984, and retrieved in January 1990. A variety of sensors and collecting devices have made possible the study of impact processes on materials of technological interest. Preliminary examination of hypervelocity impact features gives valuable information on size distribution and nature of interplanetary dust particles in low earth orbit, within the 0.5-300 micrometer size range. Most of the events detected on the trailing face of LDEF are expected to be the result of impacts of meteoritic particles only. So far, chemical investigation of craters by EDS clearly shows evidence of elements (Na, Mg, Si, S, Ca and Fe) consistent with cosmic origin. Systematic occurrence of C and O in crater residues is an important result, to be compared with the existence of CHON particles detected in P-Halley comet nucleus. Crater size distribution is in good agreement with results from other dust experiments flown on LDEF. However no crater smaller than 1.5 μm has been observed, thus suggesting a cut-off in the near earth particle distribution. Possible origin and orbital evolution of micrometeoroids is discussed. Use of thin foils detectors for the chemical study of particle remnants looks promising for future experiments.

INTRODUCTION

Interplanetary space contains solid objects whose size distribution continuously covers the interval from submicron sized particles to km sized asteroids or comets. Some meteoroids originate from comets (mainly dust ejected at perihelion), some originate from collisions within the asteroid belt. The relative contribution of these two sources is still a matter of debate. A majority of particles are likely to come from comets but recent data from the Infrared Astronomy Satellite (IRAS) indicates that asteroids could be a source larger than expected. In addition to natural particles, a significant and growing number of particles has been added by human activity in near earth space. Present knowledge of the occurrence and physical properties is based primarily on earth bound observation of meteors, comets, zodiacal light, data from infrared satellites (IRAS) as well as on board measured flux by instrumented spacecraft (Pegasus, Vega, Giotto, Space Shuttle and the MIR Soviet Space Station), study of lunar samples and dust collection in the upper atmosphere /1,2/.

The spatial density (number per unit volume) of meteoroids varies as a function of distance from the sun, distance from a planet, ecliptic latitude and longitude. The lifetime of interplanetary dust is dynamically limited, gravitational and solar radiation pressure (Poynting Roberston effect) gradually reducing the size of the orbit after typically 10^4 years; the lifetime of particles is also controlled by collision processes. Submicron particles will be blown out off the planetary system by

solar radiation pressure (β meteoroids). In the vicinity of earth, gravitational perturbations and the influence of the atmosphere greatly affect the distribution of the particles. In-situ detection and collection of dust by experiments flown on LDEF are expected to improve our current understanding of this aspect of the space environment. Originally launched for a nine month mission, the NASA Long Duration Exposure Facility (LDEF) has been retrieved after 2105 days in orbit. During its mission LDEF was stabilized with the long axis continually pointed toward the center of the earth, and surfaces perpendicular to this axis pointed at fixed angles with respect to the direction of orbital motion.

EXPERIMENTAL APPROACH

Part of the tray allocated to French experiments, known as the **FRECOPA** payload, has been devoted to the study of dust particles. The photograph (fig.1) shows the experiment in its flight configuration. The tray was located on the face of LDEF directly opposed to the velocity vector (west facing direction) in location B3 according to the LDEF description.

Two entirely passive experiments have been flown for the detection of microparticles. The first one: **Study of Meteoroid Impacts on Various Materials (AO138-1)** was composed of a set of thick glass and metallic samples; the second one: **Dust Debris Collection with Stacked Detectors (AO138-2)** was composed of multilayer thin foil detectors. The collection area was about 2000 cm². In addition to these dedicated experiments a large variety of materials on the same tray (8500 cm²) have been exposed to the bombardment of microparticles and are expected to provide additional data. Detailed description of the hardware has been given elsewhere /3,4/ and will be only summarized here. Samples of interest for both experiments are listed on tables 1 and 2.

The thick target experiment (**AO138-1**) comprises selected metallic (Al, Au, Cu, W, Stainless Steel, thickness : 250 μ m) and glass surfaces (1.5 mm thickness). Samples have been exposed to space for all the mission duration (5.5 years). Crater size distribution from these thick target experiments will enable, with the aid of laboratory calibration by solid particle accelerators, the evaluation of the incident microparticle flux in the near earth environment. Information on the velocity, particle density and incident direction will be generally difficult to decode; however this could be partially determined by studying the geometry of impact craters.

A more critical issue is the determination of the chemical composition of the impacting particles. In general they are physically destroyed and mixed with target material in the process of crater formation. Although little or no pristine material is likely to be left for chemical analysis, particularly in metals such as tungsten or gold, it is possible to collect quite sufficient projectile residue material for analysis /5/. Based on laboratory experiments such residues may be reduced to a probable initial composition.

The multiple foil penetration and collection experiment (**AO138-2**) was located inside one of the three canisters, for maximum protection of fragile thin metal films before and after exposure to space /3,4/. The canisters have been opened a short time after LDEF deployment and closed nine months later. The aim of the experiment is primarily to investigate the feasibility of multilayer thin film detectors acting as energy sorters in order to collect micrometeoroids, if not in their original shape, at least as "break-up" fragments suitable for chemical analysis. The behaviour of hypervelocity particle impacts on thin foils has been extensively studied in the laboratory and data will provide a basis for interpretation. Upon perforation of a thin foil, a particle undergoes either a deceleration or a fragmentation, depending on impact velocity, density of the target or projectile and thickness to diameter ratio /6,7/. One or more thin metallic foils are set in front of the main target in order to produce size selective detectors. Foil thickness ranges from 0.75 μ m to 5 μ m of aluminium; such foils are expected to slow down particles with diameters between 1 and 10 μ m diameter, without complete destruction. Separation distance between foils is 1 mm, enough to have eventual fragments dispersed over a large area.

PRELIMINARY RESULTS

The experiment has been recovered in good conditions after exposure to space. As a consequence of its position on LDEF, exposure to atomic oxygen erosion was kept to a minimum. In this paper we shall give results concerning the largest impact features found on the experiments and on the FRECOPA payload and some first data concerning the size distribution of small size craters. After preliminary observation by the M&D SIG team during LDEF deintegration at KSC, the FRECOPA tray has been carefully searched for impact features, at CNES prior to deintegration of experiments and at CERT. The survey was made with an optical microscope Nikon Profile Projector V12 at magnifications 20X and 100X. Scanning electron microscopy (SEM Jeol JSM-840A at CERT and Orsay) has been used for the samples purposely dedicated to the experiment and for any peculiar feature observed on other surfaces. Energy dispersive spectroscopy (EDS Link Analytical eXL analyser at CERT and EDAX Analysis Tracor system at Orsay) chemical investigation of projectile remnants has been carried out in some craters. Materials not specifically dedicated to dust detection have provided useful data, mostly because of the large area time exposure. As expected, the number of impact craters varies significantly with the location on the LDEF surface. Comparison with data from different locations on LDEF and comparison with other experiments will be made later.

Large Craters into Thick Targets

Three main types of materials have been exposed to micrometeoroid impacts: metals, fiber glass thermal covers backed by mylar foil, and quartz samples.

Two large impact features have been found : one full penetration (diameter 1.25 mm) and one marginal penetration (diameter 1.07 mm) of a 1mm aluminium shield. About 90 craters larger than 50 μm have been found on a total area of one square meter. Four craters are larger than 500 microns. Most of the large craters are circular in outline, though some small craters do indicate oblique incidence. Table 3 summarizes all the large craters found on different materials. The figures 2 to 5 show typical hypervelocity impact craters into different materials. Craters on aluminium, stainless steel and copper are typical of hypervelocity impact in metals /8/, with a depth to diameter ratio of about 0.55. Few large impacts have been found so far on quartz targets, two of them show a morphology typical of impacts on brittle materials (figure 3): a central pit with evidence of fusion, an inner ring of spalls and an outer more or less symmetrical spallation zone /9/; similar features have been found extensively on lunar samples. For the elongated shape of the central pit, it is possible that the projectile was irregularly-shaped or impacted at a large angle of incidence (greater than 45° in order to change the shape of the central pit). A number of impacts have been found on the thermal covers (tefloned glass fabric). Figure 4 shows a typical perforation. The hole diameter is approximately the same on the reverse side of the composite, as would be expected from a thin plate. Damage consists of broken fibres with missing binder material, confirming initial findings by NASA /8/. The picture shows evidence of both brittle fibre fracture and of fibre melting. Features of peculiar interest are damages caused to the mylar foil located beneath the fiber glass fabric. Under UV irradiation the mylar became very brittle and was badly damaged upon impact. This is an illustration of synergistic effects on the degradation process occurring in space.

Microcraters into Thick Targets

Four cm^2 of aluminium sample A54 from the AO138-1 experiment have been thoroughly analyzed in search of microcraters less than 20 μm in size. We used a JEOL 840 Scanning Electron Microscope, equipped with an EDAX Analysis Tracor system. The detector had no window protection allowing a quantitative analysis of elements down to $Z=23$ and a qualitative research of Carbon and Oxygen (nitrogen could not be detected with this equipment). A first scanning of the samples at a magnification of 750 X allows a selection of events showing typical crater features (circular feature, ridge). A typical flux density of a $2 \cdot 10^{-4}/\text{m}^2/\text{s}$ crater larger than 1.5 μm has been estimated; flux mass distributions found for larger craters can thus be extended with very good agreement to such small

sizes. Data are consistent with results from the IDE experiment in the same size range* We observed no craters smaller than 1.5 μm in size, thus implying a cut off in the particle size distribution, orbiting the earth and impacting our samples, a similar trend has been observed by E. Zinner¹ on another experiment . Considering simulation experiments concerning the crater diameter to particle diameter ratio, for various collector thicknesses, we can admit a factor 5 between the crater size and the particle size : the smallest impacting particles have a mass in the 10^{-13} g. region.

Microcraters into Thin Targets

Of peculiar interest was the study of impact features on the thin foil detectors. As the exposure was limited to nine months areal density of impacts is small and study is still in progress. The figure 5 shows the perforation of a 5 microns aluminium foil (sample AD11). The perforation formed an ellipse measuring 55 by 40 microns (oblique impact or elongated projectile). It is a typical "supramarginal perforation" with a crater diameter to foil thickness ratio of $D/f=10$; diameter of the particle is estimated to be 40 microns. The bottom plate beneath the perforation shows a star-shaped distribution of small secondary craters (sample AD12). The top foil acted as a shield, fragmenting the projectile and spreading the fragments over the surface of the thick plate. The craters range in size from 0.6 μm to 15 μm and are mostly distributed along two axes. An angular particle, 18 mm by 15 mm is visible at the intersection of the axes. EDS analysis has provided evidence of impactor fragment. As shown later, chemical investigation of secondary craters has given information on the composition of an impacting particle. Detectors consisting of a thin shield and thick bottom plate appear to offer a significantly higher return of information concerning chemical analysis of impactor residues than single plate detectors.

Crater Size Distribution

The cumulative flux size distribution of craters (in aluminium) larger than 30 microns is shown in the lower part of the figure 6. Several trends are visible : the flattening of the distribution at small sizes is largely an observational artifact, due to the limited resolution of optical microscopy; the middle part of the curve is consistent with the general size spectrum of microparticles and data obtained elsewhere on LDEF; the change of slope at large sizes could be an artifact due to the limited time-area of sampling, or more likely real as discussed by McDonnell et al. /10/. The upper part of the figure shows the crater size distribution of craters between 1 micron and 10 microns as derived from preliminary SEM scanning of small craters on aluminium samples (A54).

Figure 7 shows the flux, or number of particles/ m^2/s able to perforate a plate of aluminium of given thickness as derived from perforations observed on our experiments. On the figure 8 is shown a comparison between the distribution of craters observed on the Freccia experiment (A54-4/AO138) and an average value of the distribution of impact craters on the leading edge and on the trailing edge of LDEF as obtained from other experiments (S0001, MAP, IDE).[†] Agreement between A0138 data and average trailing edge data is good.

Flux Mass Distribution

The impact site survey yields a crater size distribution, which should be converted to a particle mass distribution by using the relevant relationship between crater sizes and particle mass and velocity. The discussion is out of the scope of this paper; however assuming an average impact velocity of 20 km/s, the value of the ratio of crater diameter (D) to the particle diameter (d) , could be chosen as : $D/d = 5$. Figure 9 shows the cumulative flux versus the mass of particles, as derived from AO138 dust experiments; for comparison is shown the flux derived from the Grün et al. model /11/, computed for an altitude of 500 km above the earth surface (randomly oriented plate).

The mass distribution in comparison to a review of comparable near-earth data shows a good agreement /10/; the flux on the west face of LDEF is about 10 times lower than on the east face, for

¹ E.Zinner, private communication

* J.D. Mulholland et al. LDEF Interplanetary Dust Experiment : A high time resolution snapshot of the near-earth particulate environment, in : *Proc. Hypervelocity Impact in Space*, Canterbury, 1-5 July 1991, (to be published 1992).

[†] M. Zolensky et al. Meteoroid and orbital debris record on LDEF, in : *Proc. Hypervelocity Impact in Space*, Canterbury, 1-5 July 1991, (to be published 1992).

large particles. Most of the particles impacting this west face should be interplanetary dust particles, not orbital debris. This fact is substantiated further by the chemical identification of projectile remnants inside craters.

Chemical Analysis of Particle Remnants

The first EDS X ray analysis of a few small craters has shown occurrence of elements Ca, K, Ti, Fe and S. Typical spectra are shown on figure 10. Further analysis will doubtless give an insight on the origin of the impacting objects.

A chemical analysis of all the craters found on sample A54 has been performed : X ray identification of elements down to C is possible, because the detector used in the Edax-Tracor system is window less. However nitrogen cannot be identified and of course as the collector is made of Aluminium, no information on Al is possible; semi quantitative analysis is only possible beyond Z=23 (Na).

Table 4 summarizes our results for the 15 craters identified so far : light elements C and O are present, with a ratio C/O varying from 0.1 to 3. Significant variations appear inside the distribution of individual craters. The other main elements identified in the various craters are usually referred to as "chondritic" elements, as they exist in various proportions and are signatures of extraterrestrial particles : Na, Mg, Si, S, Ca and Fe. For these elements also, important variations are found from point to point inside the crater reinforcing the idea that the particles are truly aggregates bursting apart during the impact. The systematic presence of C and O components in the various residues analyzed is an important result: the occurrence of CHON particles detected in P-Halley nucleus (PUMA and PIA experiments) would not be a particularity of this comet but could be a constant for extraterrestrial particles of cometary origin, as seems to be the case for such particles .

For the sample AD12 located beneath the thin foil perforation described earlier, the elements identified, in the central part of impact feature : Si, Fe, Na, Mg are characteristic of interplanetary dust particles from the mafic silicate family with olivine as a strong candidate. The variation in chemical composition between and within craters confirms the idea of an aggregate particle which burst apart on impact. None of the above elements were found in the outside craters (far from center of impact feature) which implies that these were caused only by aluminium fragments from the top foil.

We found no evidence of elements characteristic of orbital debris (Ti, Zn). We are thus highly confident that all the craters analysed are of extraterrestrial origin, as expected due to the fixed orientation of LDEF during its flight and to the exposition side of FRECOPA payload on board LDEF. However there is still a possibility to record impacts from orbital debris in highly eccentric orbits.† Further investigation is obviously needed.

CONCLUSION

LDEF offers a unique opportunity for the study of the many processes involved upon high velocity impact phenomena and for the comprehensive description of the LEO microparticle population. Particle collection in space will remain generally difficult, perhaps impossible for the highest meteoritic velocities. Deceleration of lower velocity particles by multiple layer foils tentatively proved sufficient to expect the retention of material suitable for identification. As shown by the preliminary investigation of experiments and materials retrieved on FRECOPA, use of opportunities to gain access to an orbiting hypervelocity impact laboratory offers considerable promise for the future. The investigation of this near-earth region of space is a necessity not just for scientific but also for technical reasons. However a great deal more research needs to be carried out to confirm the validity of the findings.

Acknowledgements : Support from CNES for completion of experiment and for data analysis and support from NASA for completion of the mission are greatly acknowledged.

† M. Zolensky et al. Meteoroid and orbital debris record on LDEF, in : *Proc. Hypervelocity Impact in Space*, Canterbury, 1-5 July 1991, (to be published 1992).

REFERENCES

1. C.Leinert and E. Grün, Interplanetary Dust, in: *Physics and Chemistry in Space*, Springer (1988) p.34.
2. J.C.Mandeville, Aragatz Mission Dust Collection Experiment., *Adv.Space Res.* 10, 3,397, (1990).
3. J.C.Mandeville, AO138-1 and AO138-2 Experiments, in: *LDEF Mission 1 Experiments*, eds L.G. Clark, W.H. Kinard, D.J. Carter, J.L. Jones, NASA SP-473, (1984) p.121.
4. J.C. Mandeville and J.A.M. McDonnell, Micrometeoroid multiple foil penetration and particle recovery experiments on LDEF, in: *Solid particles in the solar system*, ed. I. Halliday and B.A. McIntosh, D.Reidel (1980) p.395.
5. J.L. Warren, The detection and observation of meteoroid and space debris impact features on the Solar-Max satellite. *Proc XIXth Lun.Plan.Sci.Conf.* (1989) p.641.
6. J.A.M. McDonnell, Factors affecting the choice of foils for penetration experiments in space, in *Space Research X*, North Holland pub. (1970).
7. F.Hörz, Laboratory simulation of LDEF impact features, in: *First LDEF Post-retrieval symposium abstracts*, NASA CP-10072, (1991).
8. LDEF M&D SIG in: *Meteoroid and debris impact features documented on LDEF*, a preliminary report, NASA JSC, (1990).
9. J.Vedder and J.C. Mandeville, Microcraters formed in glass by projectiles of various densities, *JGR* 79,23, (1974).
10. J.A.M.McDonnell et.al. First results of particulate impacts and foil perforations on LDEF, in *Adv.Space Res.* 10, 3, XXVIII Cospar 1990, (1990).
11. E.Grün et al., Collisional balance of the meteoroid complex, *Icarus* 62,244, (1985).

Table 1 : Experiment A 0138-1 Sample List

Designation:	Material:	Thickness (microns)	Size (mm)
A1	Tungsten	150	100 x 100
A2	Aluminium	250	"
A3	Copper	125	"
A4	Steel	250	"
A5	Aluminium	250	"
A6	Aluminium/Kapton	50	"
B1 to B27	Glass	1.9 mm	diam: 25

Table 2 : Experiment A 0138-2 Sample List

Designation:	Material:	Thickness (microns)	Size (mm)
D1 - D5	Aluminium	125 5	40 x 40
D6	Aluminium	125	"
D7 - D8	Aluminium	125 2 2	"
D9 - D11	Aluminium	125 5 2	"
D12	Aluminium	125	"
E1 - E3	Gold Aluminium	125 2	30 x 30
E3 - E6	Aluminium	125 2 2	"
E7 - E9	Aluminium	125 0.75 0.75	"
E10 - E12	Gold Aluminium	125 0.75	"
E13 - E14	Gold	125	"
E15 - E17	Gold Aluminium	125 2 0.75	"
E18 - E19	Aluminium	125	"

Table 3

ao138cral					
Identification	Diameter, um	Depth, um	P/D	Material	Comments
1	es11	215,000			fg
2	es110	80,000			fg
3	es12	250,000			fg
4	es13	350,000			fg
5	es14	250,000			fg
6	es15	150,000			fg
7	es16	250,000			fg
8	es17	200,000			fg
9	es18	180,000			fg
10	es19	90,000			fg
11	es21	350,000			fg
12	es22	250,000			fg
13	es23	400,000			fg
14	es24	300,000			fg
15	es25	250,000			fg
16	e31	350,000			Al
17	e32	192,000			Al
18	e33	147,000			Al
19	e34	320,000			Al
20	e35	198,000			Al
21	e36	510,000			Al
22	e37	160,000			Al
23	e38	80,000			Al
24	e39	135,000			Al
25	e310	58,000			Al
26	e311	148,000			Al
27	e312	72,000			Al
28	e41	315,000			Al
29	e42	108,000			Al
30	e43	80,000			Al
31	e44	75,000			Al
32	e45	130,000			Al
33	e46	200,000			Al
34	e51	1250,000			Al perf. 1 mm
35	e52	1070,000	920,000	0.860	Al
36	e53	395,000	240,000	0.608	Al
37	e54	320,000	190,000	0.594	Al
38	e55	125,000			Al
39	e56	175,000			Al
40	e57	200,000			Al
41	e58	165,000			Al
42	e59	140,000			Al
43	e510	55,000			Al
44	e511	115,000			Al
45	e512	75,000			Al
46	mv51	375,000			fg
47	ca11	142,000	65,000	0.458	Al
48	ca21	48,000			Al
49	ca31	155,000	80,000	0.516	Al
50	ca32	199,000	110,000	0.553	Al
51	ca41	225,000	130,000	0.578	Al
52	ca42	60,000	40,000	0.667	Al
53	a21	176,000	90,000	0.511	Al
54	a22	158,000	80,000	0.506	Al
55	a23	165,000	90,000	0.545	Al
56	a31	127,000	70,000	0.551	Qu
57	a41	64,000	35,000	0.547	ss
58	a42	49,000	22,000	0.449	ss
59	a51	550,000			Al perf 250 um
60	a52	55,000	30,000	0.545	Al
61	a53	50,000			Al
62	a54	100,000	65,000	0.650	Al
63	a55	62,000	35,000	0.565	Al
64	a56	36,000			Al
65	a61	50,000			kapton/Al
66	d11	60,000			Al perf 5k um
67	b251	330,000	180,000	0.545	Al
68	b261	320,000	170,000	0.531	Al
69	a24	75,000	35,000	0.467	Al
70	a11	50,000	15,000	0.300	W
71	b15	180,000			quartz pit = 30
72	b16	400,000			quartz pit= 95
73	ds1	65,000			Al
74	ds2	110,000			Al

LDEF AO138-1 SAMPLE A54-2,4 : CHEMISTRY

Crater n°	Size, μm	C/O (a)	Na	Mg	Si	S	Ca	Fe	Ni	(c)
1	1.5	1-1.5	ϵ	ϵ	ϵ					
2	1.5	0.5	ϵ		1					
3	1.5	0.7		0.2	1					
4	1.5	0.5-1			1				5	
5	2	(b)			ϵ				1	
6	2.5	1.5-3		0.17	1					
7	3	1-2	ϵ	ϵ	1					
8	3	(b)	0.3	1	(d)	1	1			
9	3.5	1			1					
10	4	0.3-04	0.4	0.2	1	ϵ	0.5	3		
11	4	0.5	ϵ	ϵ	1	ϵ	ϵ	ϵ		
12	5.5	0.5		0.1	1		0.3			
13	6	0.2		1.6	1	5	3			
14	10	0.1-1	ϵ		1		ϵ			
15	10	0.5	0.13	0.07	1	0.13	0.3	8		

Notes :

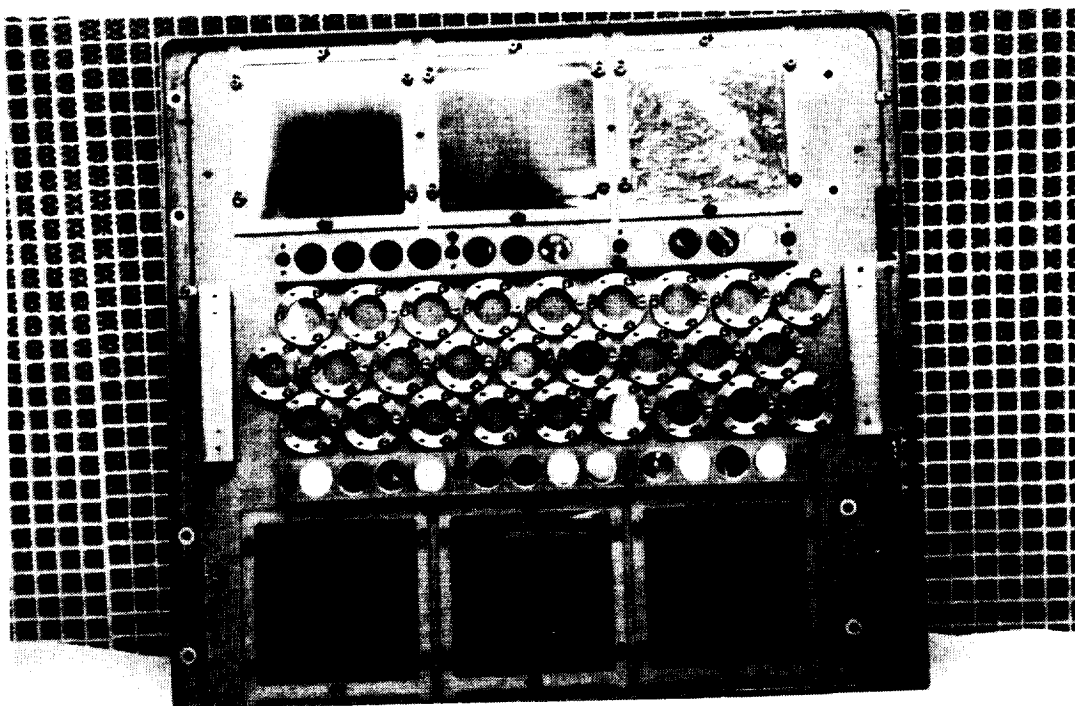
(a) : peak height

(b) : no C present

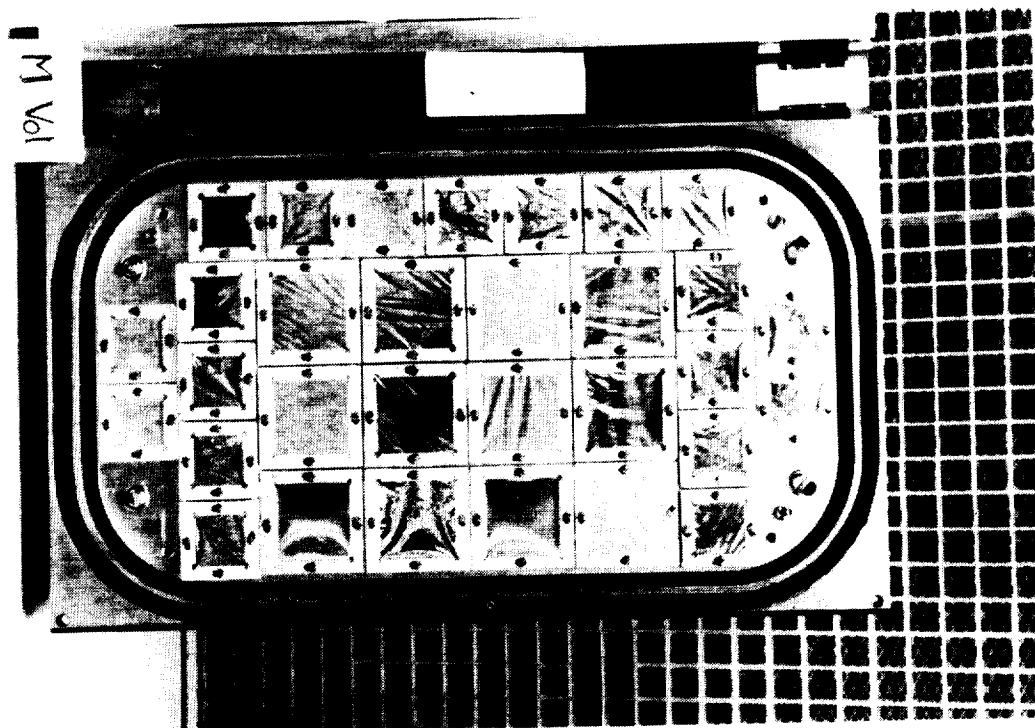
(c) : reported to (Si) =1; ϵ : very weak peak

(d) : no Si present ; reported to (Mg) = 1

Table 4



A0138-1 Experiment



A0138-2 Experiment

Fig.1. This figure shows the FRECOPA experiment tray on LDEF, one of the dust experiment is shown on the upper middle part of the tray, the other one is located inside one of the cannisters (closed upon recovery).

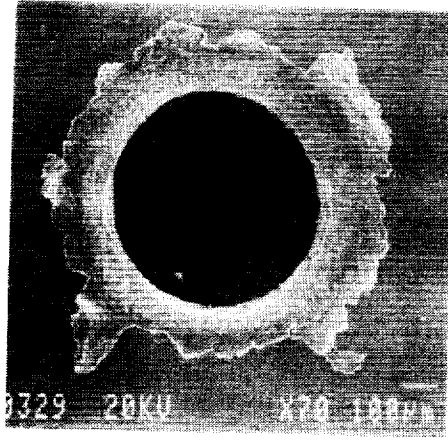


Fig.2. This figure shows a typical medium sized impact on aluminium surface.



Fig.3. This figure shows an impact crater on quartz sample.



Fig.4. This figure shows a typical crater on tefloned fiber glass fabric.

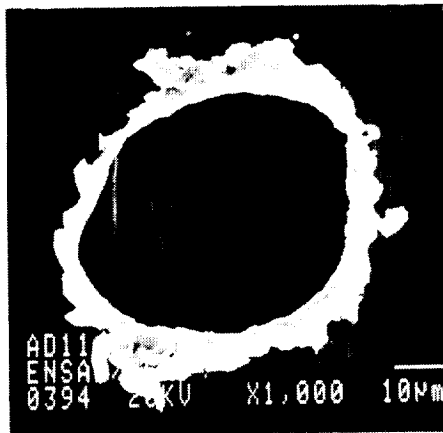


Fig.5. Perforation of a 5 microns thick aluminium foil.

ORIGINAL PAGE
BLACK AND WHITE PHOTOGRAPH

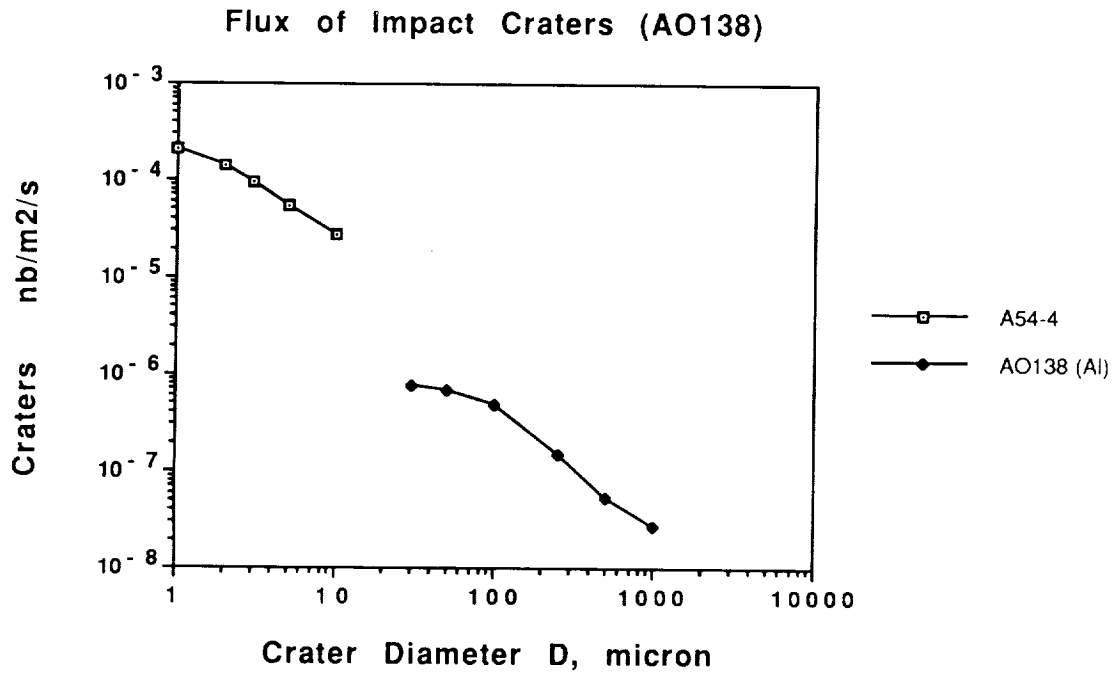


Fig.6. Cumulative flux size distribution of craters on AO138-1 and AO138-2

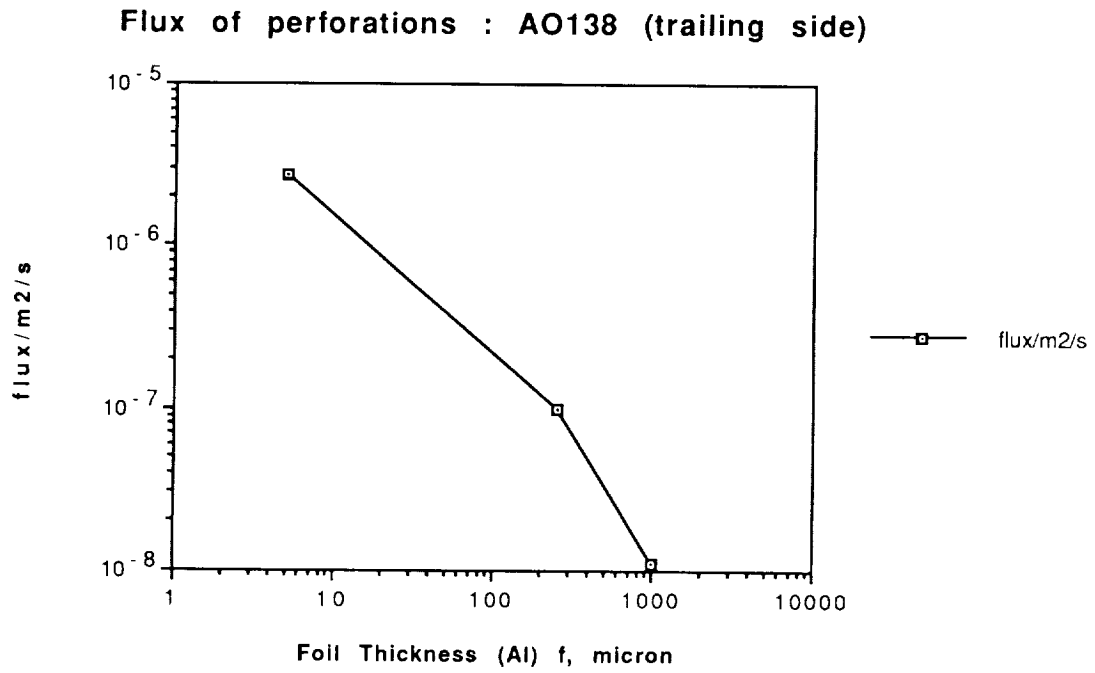


Fig.7. Flux of perforating particles.

Crater Fluence : Comparison with AO138

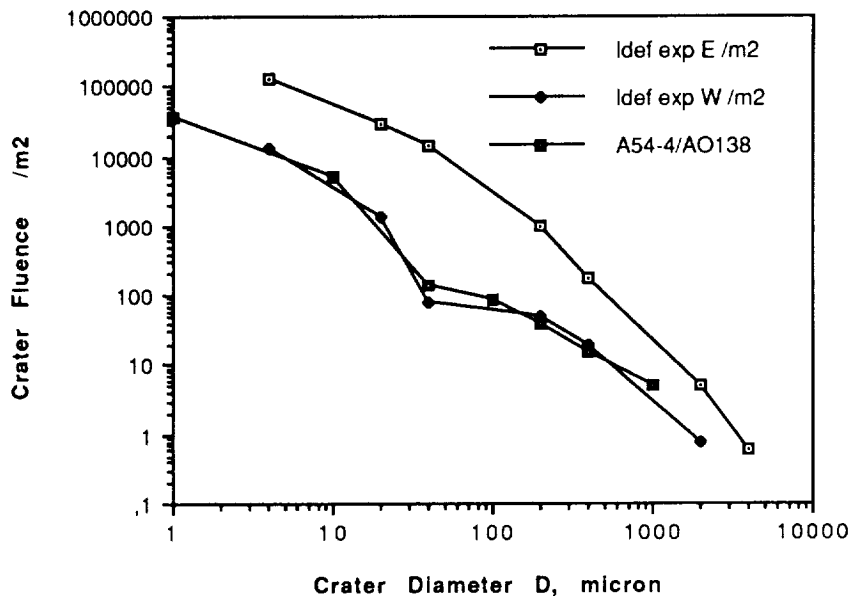


Fig.8. Comparison of crater fluences observed on FRECOPA with data from other dust experiments on LDEF.

Comparison Flux Model (Grün) and AO138

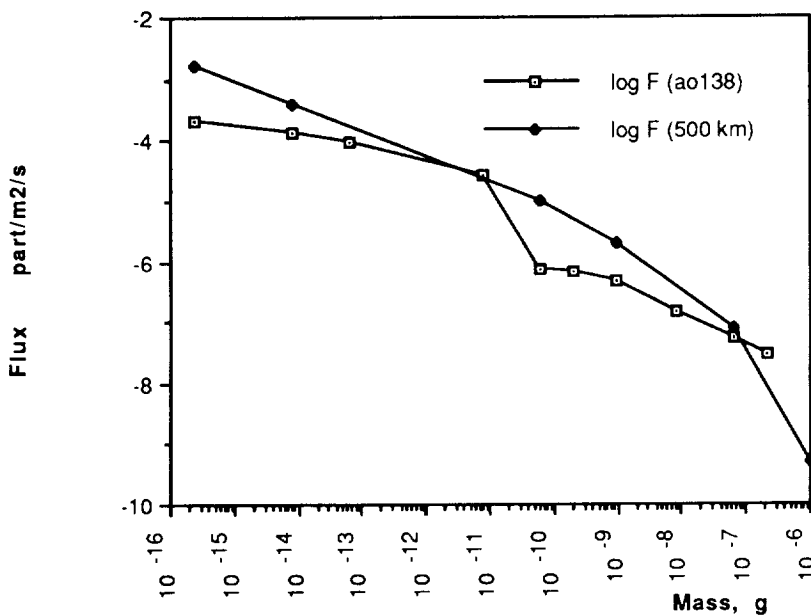
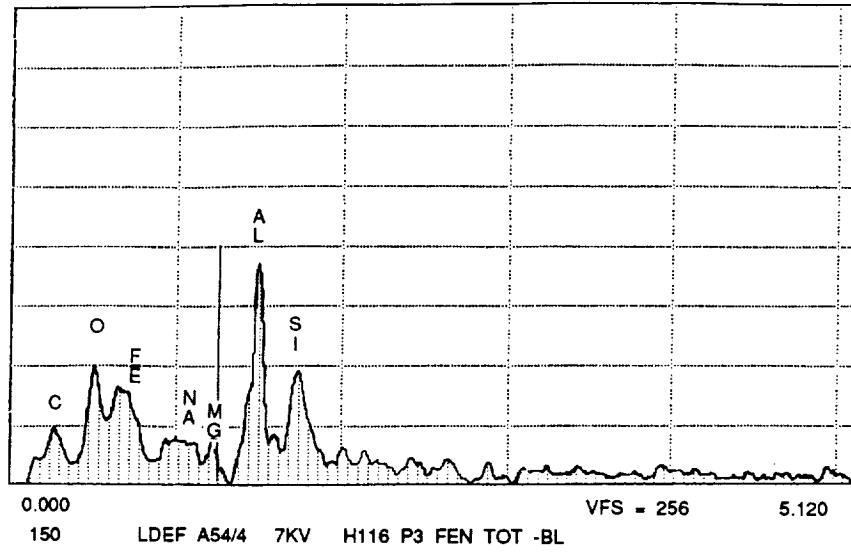


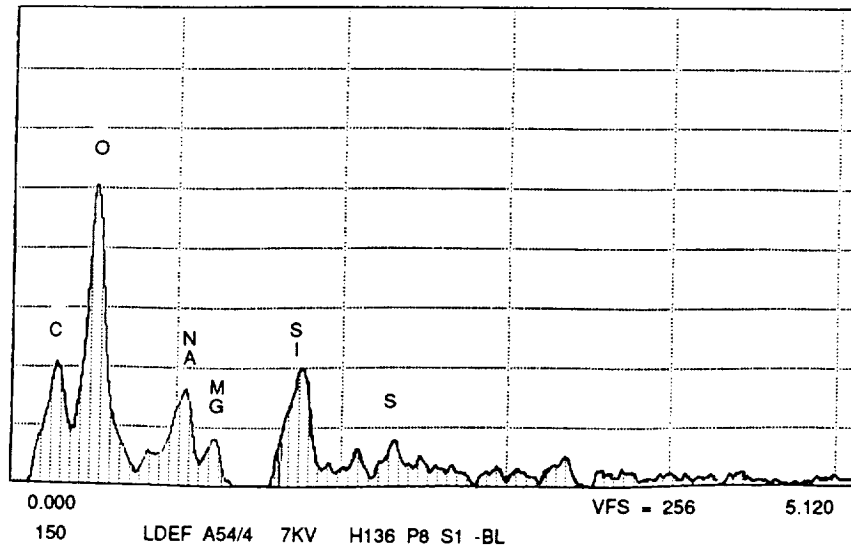
Fig.9. Cumulative flux on trailing side of LDEF as compared with flux model from Grün et al.(1985), see ref.13.

TRACOR * I.E.F.* - CEETAM - MON 18-FEB 91 09:37
CURSOR: 0.000KEV = 0



SQ: TRASH

TRACOR * I.E.F.* - CEETAM - MON 18-FEB 91 11:02
CURSOR: 0.000KEV = 0 ROI (4) 0.000: 0.000



SQ: TRASH

Fig.10. These figures shows typical X-ray spectra of points located inside impact craters